Journal of

Particle Science and Technology

J | P | S | T

jpst.irost.ir

A new precursor for preparation of magnetite (Fe$_3$O$_4$) nanoparticles
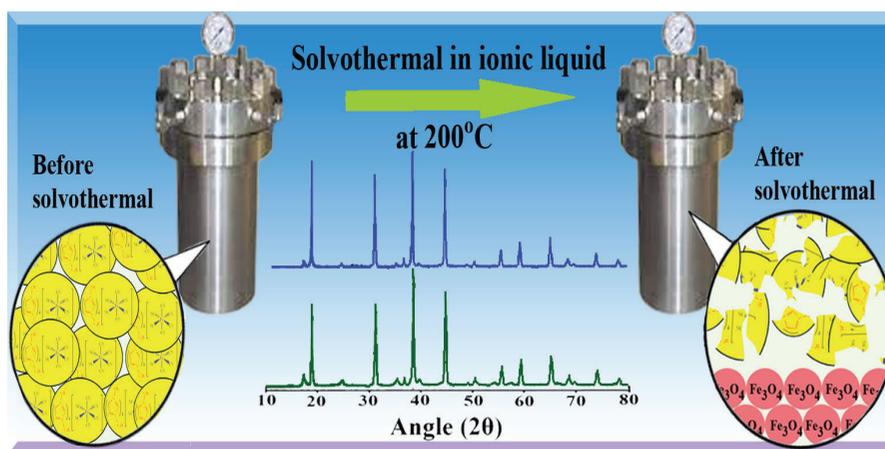
Mohammad Kaikhosravi, Hassan Hadadzadeh*, Mohammad-Taghi Behnamfar

Department of Chemistry, Isfahan University of Technology, Isfahan 84156-83111, Iran

HIGHLIGHTS

- A new precursor, (BMIM)$_4$[Fe(CN)$_6$], was synthesized for preparation of nanomagnetite.

- The precursor was prepared in ionic liquid [BMIM][PF$_6$].

- The magnetite nanoparticles were prepared by hydrothermal and solvothermal methods.

- A high purity nanomagnetite was obtained via the solvothermal method.

- The effect of solvothermal time on structure and size of nanomagnetite was investigated.

GRAPHICAL ABSTRACT

ARTICLE INFO

ABSTRACT

An anionic Fe(II) complex, (BMIM)$_4$[Fe(CN)$_6$] (where BMIM is 1-butyl-3-methylimidazolium), was synthesized in ionic liquid [BMIM][PF$_6$] under reflux condition. The complex was characterized by elemental analysis and spectroscopic methods. The magnetite (Fe$_3$O$_4$) nanoparticles were prepared by the hydrothermal and solvothermal (in ionic liquid [BMIM][PF$_6$]) methods from (BMIM)$_4$[Fe(CN)$_6$] as a precursor. The nanoparticles were characterized by X-ray diffraction (XRD), FT-IR, and scanning electron microscopy (SEM). The results show that the preparation of magnetite using the solvothermal method in [BMIM][PF$_6$] has more advantages over the hydrothermal method such as smaller size and higher purity.

* *Corresponding author. Tel.: +98 3133913240; fax: +98 3133912350.*
E-mail address: hadad@cc.iut.ac.ir (H. Hadadzadeh).

1. Introduction

Ionic liquids (ILs) are a class of salts which are liquid at ambient conditions because they have a significantly lower symmetry. Furthermore, the charge of its cation and anion is distributed over a larger volume of the molecule by resonance (Fig. 1) [1]. Generally, ILs are composed of organic cations and organic or inorganic anions (Scheme 1). The most prominent IL cations include alkylammonium, alkylphosphonium, N,N-dialkylimidazolium, and N-alkylpyridinium cations (Scheme 2). The IL anions are chloride, bromide, iodide, $[BF_4]^-$, $[AlCl_4]^-$, $[PF_6]^-$, and $[SbF_6]^-$. ILs have specific physical properties such as thermal stability, low vapor pressure, electric conductivity, interesting solvent properties, biphasic systems possible, liquid crystalline structures, high electroelasticity, high heat capacity, and non-flammability [2-6]. These unique properties make ILs attractive for scientists in a variety of field such as: electrochemical sensors and biosen sors [7,8], engineering [9,10], membrane [11], catalysts [10,11], and synthesis of nanostructures [14-17]. In the synthesis methods of nanostructures, the control of morphology is very important for researchers. So, using of ILs in the solvothermal method is a good choice for this control.

Recently, we have been interested in the use of new precursors for the preparation of nanoparticles. In this study, the magnetite nanoparticles were prepared via hydrothermal and solvothermal methods from a new anionic Fe(II) complex, $(BMIM)_4[Fe(CN)_6]$ (where BMIM is 1-butyl-3-methylimidazolium), as a precursor. The effects of several parameters such as reaction time, solvent and temperature on the size and morphology of the magnetite nanoparticles were also investigated. In comparison with the reported methods for the preparation of magnetite nanoparticles, our proposed method is simple, fast, low-cost without using any special instruments, and does not require high-temperature operation.
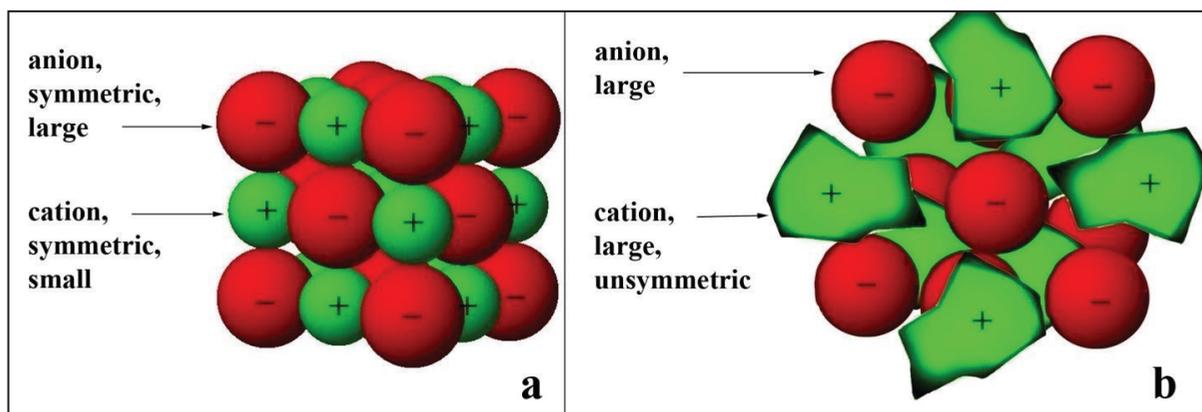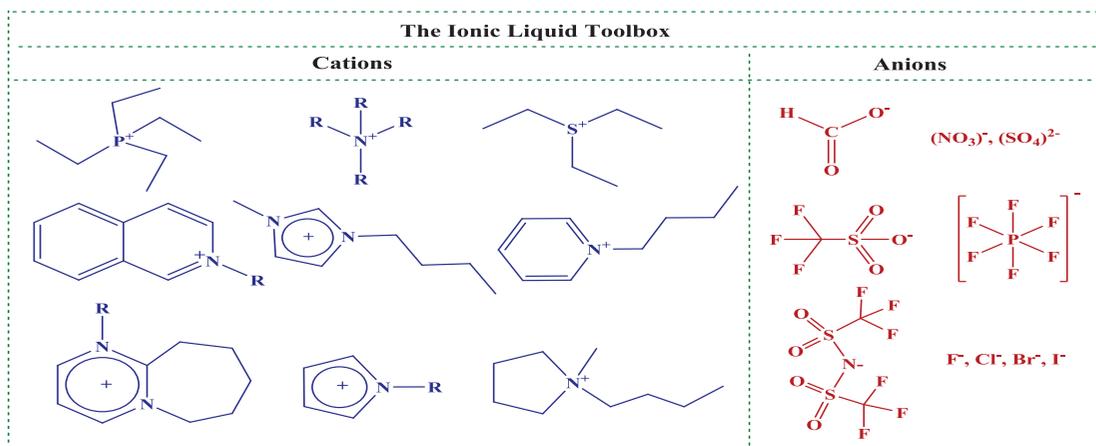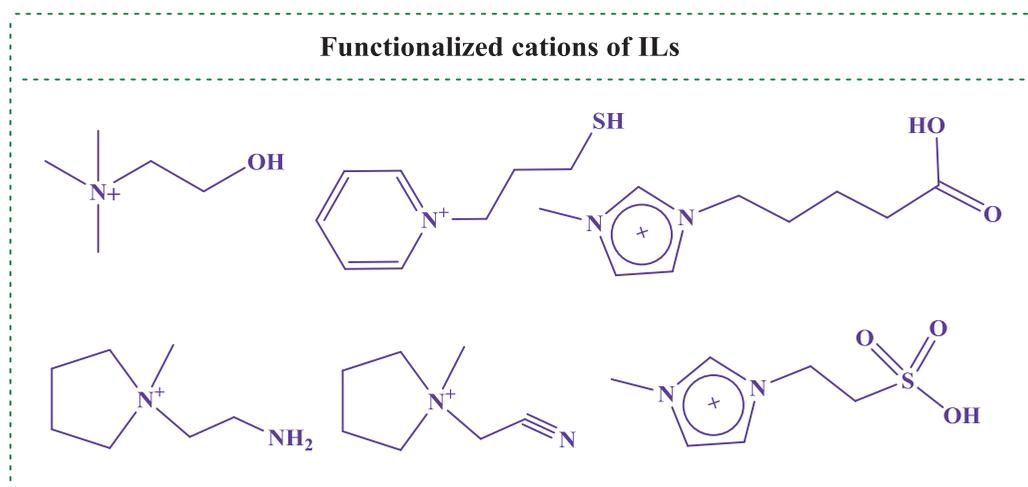

Fig. 1. Charge distribution in common salts (a) and ILs (b).

Scheme 1. The ionic liquid toolbox: important model cations and anions for ILs.

Functionalized cations of ILs

Scheme 2. Functionalized cations of ILs.

2. Experimental

2.1. Materials and methods

All chemicals and solvents were reagent grades from Merck and used without any further purification. Elemental analyses were performed by using a Leco, CHNS-932 elemental analyzer. FT-IR spectra were recorded on an FT-IR JASCO 460 spectrophotometer in the region of 4000–400 cm⁻¹ using KBr pellets. Electronic absorption spectra were recorded on a JASCO 7580 UV–Vis–NIR double-beam spectrophotometer. Quartz cuvettes of 10 mm path length were used for spectrophotometric experiments. XRD patterns were recorded by a Philips, X-ray diffractometer using Ni-filtered Cu Kα radiation. The morphology of the nanoparticles was observed using FE-SEM (HITACHI; S-4160). Prior to taking images, the samples were coated by a very thin layer of Au to make the sample surface conducting and prevent charge accumulation, and obtaining a better contrast.

2.2. Synthesis of $(BMIM)_4[Fe(CN)_6]$

In the first step, a mixture of NaCN (0.05 g, 1mmol) and tetra-n-butylammonium bromide (TBAB) (0.32 g, 1mmol) was dissolved in 20 mL methanol and stirred for 1 h at room temperature. The white precipitate, tetra-n-butylammonium cyanide (TBACN), was filtered, washed with methanol and dried in air. In the second step, $FeCl_2 \cdot 6H_2O$ (0.28 g, 1 mmol) was added to tetra-n-butylammonium cyanide (TBACN) (0.27 g, 1 mmol) in 5 mL ionic liquid [BMIM][PF$_6$] and refluxed for 10 h. The resulting yellow precipitate,

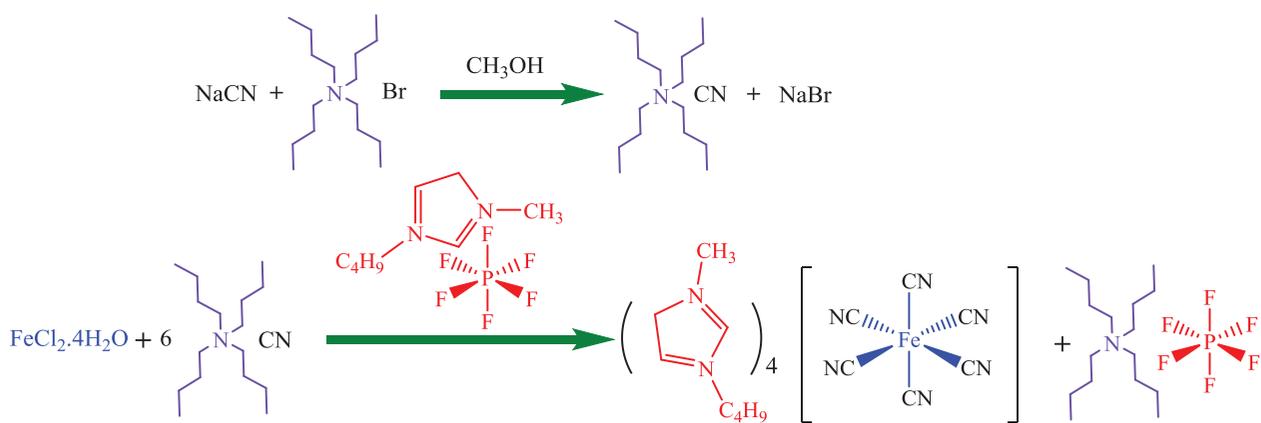$(BMIM)_4[Fe(CN)_6]$, was filtered and washed with water/acetone mixture (1:1), and then air dried at ambient temperature (Scheme 3), Yield: 0.5 g, 65%.

2.3. Preparation of the magnetite nanoparticles by solvothermal method in ionic liquid [BMIM][PF$_6$]

The precursor complex, $(BMIM)_4[Fe(CN)_6]$, (0.4 g) was added to 5 mL ionic liquid [BMIM][PF$_6$] and stirred for 2 h. The reaction mixture was transferred to a 10 mL Teflon-lined autoclave and heated in an oven at 200˚C for three different times of 12 h, 24 h and 36 h. The resulting product was centrifugated at 3000 rpm, washed with ethanol and water to remove any impurities, and dried in an oven at 80˚C overnight. (Fig. 2).

2.4. Preparation of the magnetite nanoparticles by hydrothermal method

$(BMIM)_4[Fe(CN)_6]$, (0.4 g) was added to 5 mL water and stirred for 1 h. The reaction mixture was transferred to a 10 mL Teflon-lined autoclave and heated in an oven at 200˚C for 12 h. The resulting precipitate was centrifugated, washed with water, and dried in an oven at 80˚C overnight.
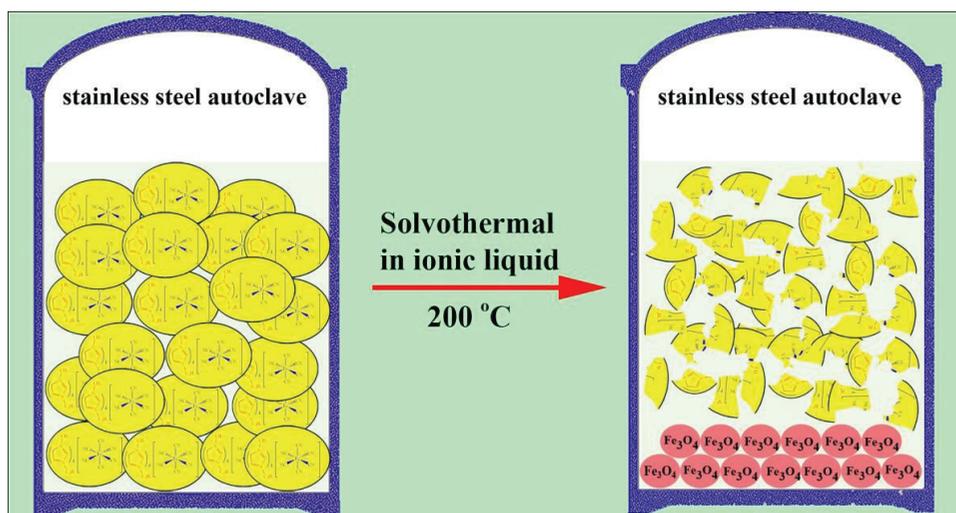
Scheme 3. Synthesis route to (BMIM)$_4$[Fe(CN)$_6$].

Fig. 2. Preparation of the magnetite nanoparticles in [BMIM][PF$_6$].

3. Result and discussion

The synthesis route to (BMIM)$_4$[Fe(CN)$_6$] is shown in Scheme . 3. Due to the poor solubility of NaCN in the ionic liquid ([BMIM][PF$_6$]), the sodium salt was changed into tetra-n-butylammonium salt. The reaction between FeCl$_2$·6H$_2$O and TBACN in refluxing [BMIM][PF$_6$] gave (BMIM)$_4$[Fe(CN)$_6$] in 65% final yield. Elemental analysis of the complex was entirely consistent with its proposed composition. The complex has good solubility in acetonitrile, DMF, and DMSO. Also, (BMIM)$_4$[Fe(CN)$_6$] is stable in the solid as well as in solution.

The magnetite nanoparticles were prepared by two different methods vis hydrothermal and solvothermal in [BMIM][PF$_6$] (Fig. 2).

The FT-IR spectrum of the complex shows typical bands associated with (CN$^-$) ligand coordinated to Fe(II). The C–H stretching vibration bands of the aliphatic hydrogen of BMIM counter ions are appeared around 2900–3100 cm^{-1}. The band at 593 cm^{-1} is assigned to the υ(Fe–C) vibration.

The cyanide anion can coordinate to a metal atom in two different modes, viz. monodentate (M–CN), and bridging mode (M–CN–M›, M = or ≠ M›). The IR stretching bands of the coordinated cyano ligand appear in the range of 2025–2200 cm^{-1}, while the bands are generally observed at 2025, 2044, and 2070 cm^{-1} for a monodentate mode (M–CN). For the bridging mode, the υ(C≡N) is higher by 40–100 cm^{-1} than that of the monodentate mode in [Fe(CN)$_6$]$^{4-}$ ion. If the complex structures are similar, this rule is very useful [3]. In (BMIM)$_4$[Fe(CN)$_6$], the band at 2055 cm^{-1} corresponds to υ(C≡N) of the monodentate cyano ligands. The broad absorption band at 3446 cm^{-1} is attributed to the υ(OH) vibration of the crystallization water molecules. [18] (Fig. 3).
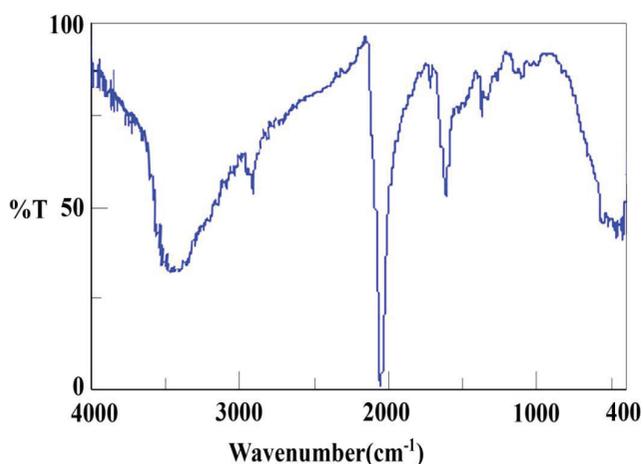
Fig. 3. FT-IR spectrum of $(BMIM)_4[Fe(CN)_6]$.

The FT-IR spectra of the magnetite nanoparticles in different times (12 h (a), 24 h (b), and 36 h (c), in ionic liquid, and 12 h (d) in water) at 200°C are shown in Fig. 4. In the case of solvothermal method in [BMIM] $[PF_6]$, the band associated with the CN^- ligand at 2055 cm^{-1} is decreased from (a) to (c), indicating the amount of the cyano ligand is decreased with increasing the solvothermal reaction time. In contrast, when the water solvent was used for the hydrothermal method, the band associated with the cyano ligand is appeared at 2055 cm^{-1}. In this method, some carbonate salts were produced as a by-product. The carbonate vibration is appeared at 1050 cm^{-1}. The vibrations at about 450 and 750 cm^{-1} are attributed to the stretching vibration of the Fe–O bonds [18-20] (Fig. 4).

The electronic spectrum of the complex was recorded in acetonitrile. The d^6 hexacyano complexes display very simple electronic spectra. In view of the large LF strength of the cyano ligand, the t_{2g}—e_g interval is very large, and the cyano complexes are low-spin. LMCT transitions, from lower lying CN states, must terminate on the high energy eg level because the t_{2g} level is full of electrons. Such transitions will generally fall beyond 200 nm. In the electronic spectrum of $[Fe(CN)_6]^{4-}$, there is a broad MLCT band in the UV–Vis region, namely $t_{2g} \rightarrow t_{1u}$ MLCT and $t_{2g} \rightarrow t_{2u}$ MLCT (Fig. 5). In this complex, since the ground state is $^1A_{1g}$, only transitions to $^1T_{1u}$ are fully allowed [21].
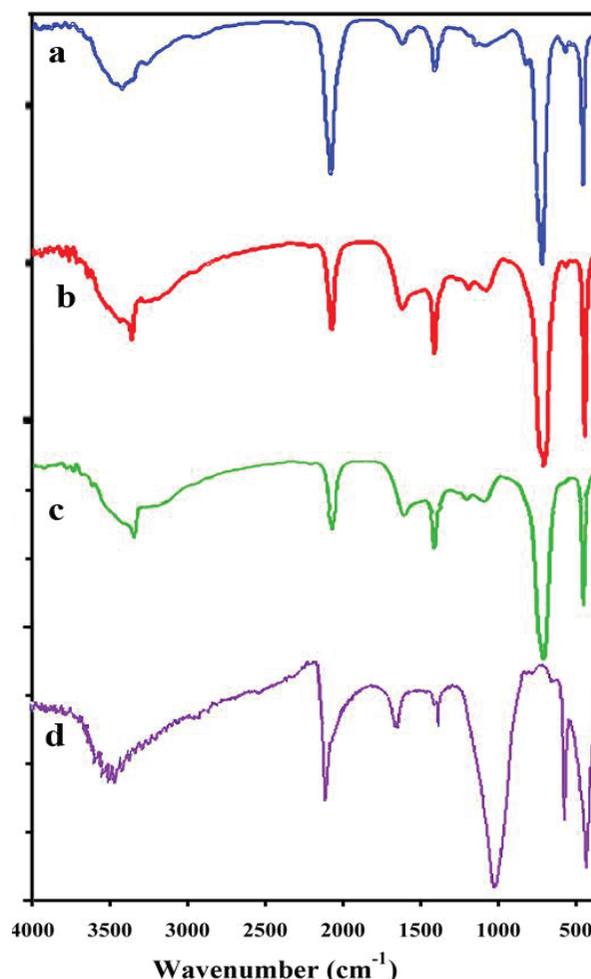

Fig. 4. FT-IR spectra of the prepared magnetite nanoparticles by two methods; solvothermal in different times: 12 h (a), 24 h (b), 36 h (c), and hydrothermal for 12 h (d) at 200°C.

Fig. 5. UV-Vis spectrum of $(BMIM)_4[Fe(CN)_6]$ in CH_3CN.

3.3. XRD analysis

The X-ray diffraction pattern of the magnetite nanoparticles is shown in Fig. 6. The diffraction patterns show that the nanoparticles have a crystalline morphology and haven't any amorphous phase at their structures. The solvothermal reaction of $(BMIM)_4[Fe(CN)_6]$ in $[BMIM][PF_6]$ in three different times: 12h (Fig. 6, a), 24 h (Fig. 6, b), and 36 h (Fig. 6, c) at a 200°C resulted the magnetite crystalline phase, which is in agreement with the literature [19,20]. As shown in Fig. 6, the XRD pattern of the nanoparticles reveals that the diffractogram can be determined as Fe_3O_4 with a cubic phase, which can be filed to (220), (311), (400), (422), (511) and (440) planes (JCPDS Card No. 082–1533).

Fig. 6. XRD patterns of the prepared magnetite nanoparticles by two methods; solvothermal in different times: 12 h (a), 24 h (b), 36 h (c); and hydrothermal for 12 h (d) at 200˚C.
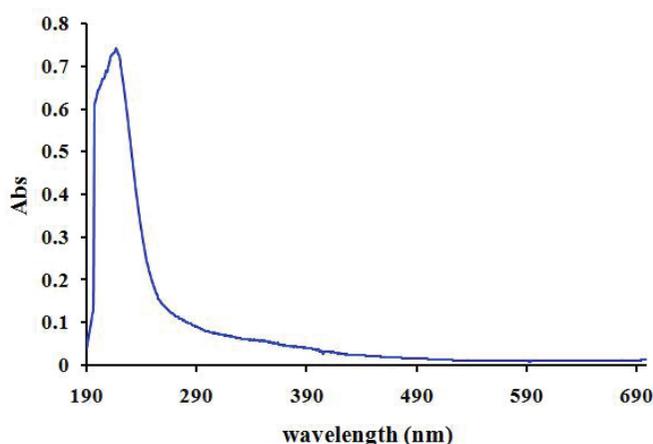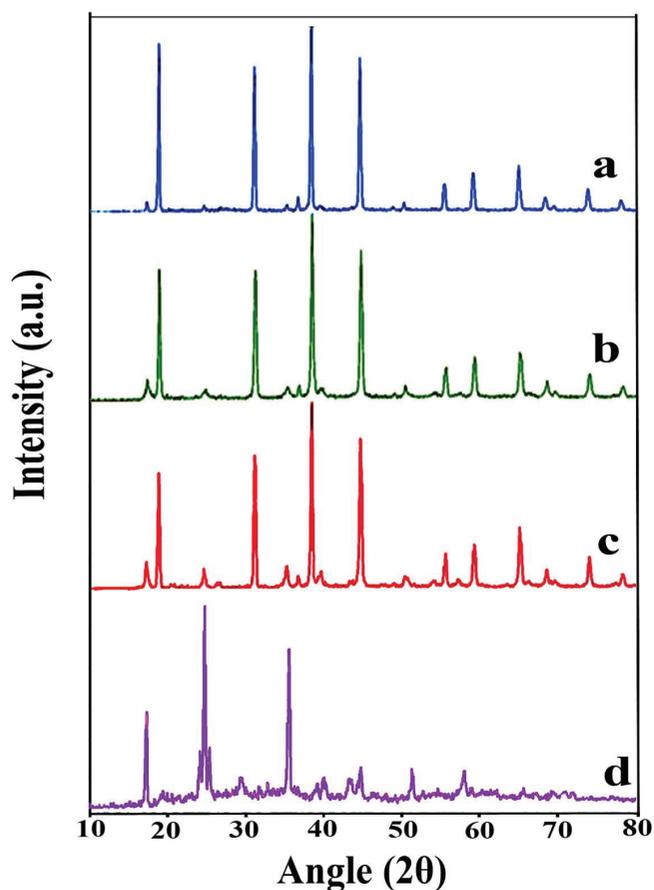
The crystallite size (Dc) of the magnetite nanoparticles was calculated to be 25 nm using the Debye–Scherrer equation [22], which is in agreement with that observed from the FE-SEM images.The crystallite size was calculated using the most intensity peaks.

Fig. 6d shows the typical XRD patterns of the magnetite nanoparticles prepared by the hydrothermal method at 200°C for 12 h. The reflection peaks can be readily indexed to the crystalline phases. In comparison to the solvothermal method in $[BMIM][PF_6]$, several peaks for the carbonate by-product are seen in this pattern. The crystallite size (Dc) of the nanoparticles was calculated to be 47 nm.

3.4. FE-SEM studies

The morphological images of the magnetite nanoparticles were studied by FE-SEM technique. According to the FE-SEM images, the morphology of the magnetite nanoparticles has the small fragment size and the nanoparticles are formed with irregular shapes. The particle size of the magnetite nanoparticles is between 15–50 nm (Fig. 7).
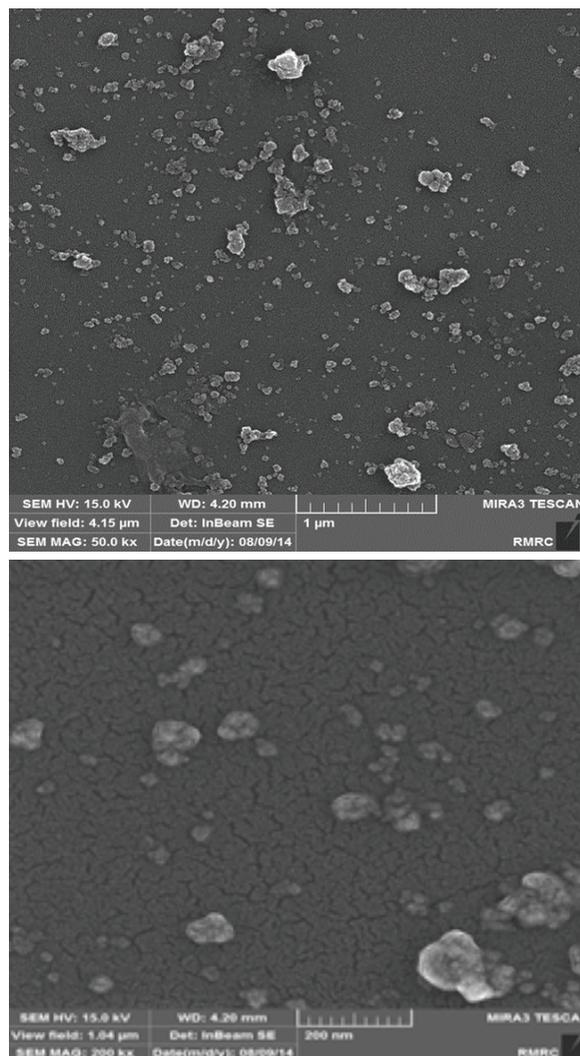

Fig. 7. SEM images of the prepared magnetite nanoparticles by the solvothermal method for 24 h at 200˚C.

4. Conclusions

For the first time, a mononuclear Fe(II) complex with bulky counter ions, (BMIM)$_4$[Fe(CN)$_6$], has been synthesized in an ionic liquid with a good yield. We have also synthesized and characterized the pure magnetite (Fe$_3$O$_4$) nanoparticles via a fast and facile solvothermal method in an ionic liquid. The effect of time on the structure and grain size of the magnetite nanoparticles was investigated. In comparison to the hydrothermal method, the results reveal that the preparation of magnetite using the solvothermal method in [BMIM][PF$_6$] yields pure and smaller nanoparticles. In hydrothermal method, the final product was impure and its XRD pattern revealed several peaks for carbonate as a by-product.

Acknowledgements

References

[1] J. D. Holbrey and K. R. Seddon, Ionic Liquids, Clean Technol. Environ. Policy. 1 (1999) 223–236.

[2] C. Method, M. S. T. Mahmoudi, CeO$_2$ nanoparticles synthesized by a microwave-assisted hydrothermal method: evolution from, J. Clust. Sci. 23 (2012) 597–602.

[3] R. M. Cornell, U. Schwertmann, The iron oxides: structure, properties, reactions, occurrence and uses, WILEY-VCH, New York, 1996.

[4] X. Wang, Y. Chi, and T. Mu, A review on the transport properties of ionic liquids, J. Mol. Liq. 193 (2014) 262–266.

[5] D. Santos, F. Costa, E. Franceschi, A. Santos, C. Dariva, S. Mattedi, Synthesis and physico-chemical properties of two protic ionic liquids based on stearate anion, Fluid Phase Equilib. 376 (2014) 132–140.

[6] J. M. P. França, F. Reis, S. I. C. Vieira, M. J. V. Lourenço, F. J. V. Santos, C. A. Nieto de Castro, A. A. H. Pádua, Thermophysical properties of ionic liquid dicyanamide (DCA) nanosystems, J. Chem. Thermodyn. 79 (2014) 248–257.

[7] A. Salimi, M. Kurd, H. Teymourian, R. Hallaj, Highly sensitive electrocatalytic detection of nitrite based on SiC nanoparticles/amine terminated ionic liquid modified glassy carbon electrode integrated with flow injection analysis, Sens. Actuators. B. 205 (2014) 136–142.

[8] V. V. Singh, A. K. Nigam, A. Batra, M. Boopathi, B. Singh, and R. Vijayaraghavan, Applications of Ionic Liquids in Electrochemical Sensors and Biosensors, Int. J. Electrochem. 2012 (2012) 1–19.

[9] W. Beichel, U. P. Preiss, S. P. Verevkin, T. Koslowski, I. Krossing, Empirical description and prediction of ionic liquids ' properties with augmented volume-based thermodynamics, J. Mol. Liq. 192 (2014) 3–8.

[10] M. Usula, E. Matteoli, F. Leonelli, F. Mocci, F. C. Marincola, L. Gontrani, S. Porcedda, Thermo-physical properties of ammonium-based ionic liquid+N-methyl-2-pyrrolidone mixtures at 298.15K, Fluid Phase Equilib. 383 (2014) 49–54.

[11] S. H. Barghi, M. Adibi, D. Rashtchian, An experimental study on permeability, diffusivity, and selectivity of CO$_2$ and CH4 through [bmim][PF6] ionic liquid supported on an alumina membrane: Investigation of temperature fluctuations effects, J. Memb. Sci. 362 (2010) 346–352.

[12] C. Oumahi, J. Lombard, S. Casale, C. Calers, L. Delannoy, C. Louis, X. Carrier, Heterogeneous catalyst preparation in ionic liquids: Titania supported gold nanoparticles, Catal. Today. 235 (2014) 58–71.

[13] G. Shi, Z. Wang, J. Xia, S. Bi, Y. Li, F. Zhang, L. Xia, Y. Li, Y. Xia, L. Xia, Mixed ionic liquids/graphene-supported platinum nanoparticles as an electrocatalyst for methanol oxidation, Electrochim. Acta. 142 (2014) 167–172.

[14] S. García, J. J. Buckley, R. L. Brutchey, S. M. Humphrey, Effect of microwave heating on the synthesis of rhodium nanoparticles in ionic liquids, Inorg. Chim. Acta. 422 (2014) 65–69.

[15] M. Padervand, M. Vossoughi, Fabrication and antibacterial performance of Ag–Au nanoparticles decorated ionic liquid modified magnetic core-analcime shell microspheres, J. Environ. Chem. Eng. 2 (2014) 1989–1995.

[16] K. T. P. Charan, N. Pothanagandhi, K. Vijayakrishna, A. Sivaramakrishna, D. Mecerreyes, B. Sreedhar, Poly(ionic liquids) as "smart" stabilizers for metal nanoparticles, Eur. Polym. J. 60 (2014) 114–122.

[17] S. Rabieh, M. Bagheri, M. Heydari, E. Badiei, Microwave assisted synthesis of ZnO nanoparticles in ionic liquid [Bmim]cl and their photocatalyticinvestigation, Mater. Sci. Semicond.

Process. 26 (2014) 244–250.

[18] K. Nakamato, Infrared and Raman Spectra of Inorganic and Coordination Compounds. Part II: Application in Coordination, Organometallic and Bioinorganic Chemistry, 5th ed., Wiley-Interscience, New York, 1997.

[19] J. Sun, S. Zhou, P. Hou, Y. Yang, J. Weng, X. Li, M. Li, Synthesis and characterization of biocompatible Fe_3O_4 nanoparticles, J. Biomed. Mater. Res., Part A. 80 (2007) 333–341.

[20] Y. Wei, B. Han, X. Hu, Y. Lin, X. Wang, X. Deng, Synthesis of Fe_3O_4 nanoparticles and their magnetic properties, Procedia Engineering. 27 (2012) 632–637.

[21] A.B.P. Lever, Inorganic Electronic Spectroscopy, Elsevier, Amsterdam, 1984.

[22] R. Jenkins, and R. L. Snyder, Introduction to X-ray Powder Diffractometry, Wiley, New York, 1996.